Solar Energy Materials and Solar Cells 200 (2019) 109935

Contents lists available at ScienceDirect

Solar Energy Materials and Solar Cells

journal homepage: www.elsevier.com/locate/solmat

Design of MtNS/SA microencapsulated phase change materials for enhancement of thermal energy storage performances: Effect of shell thickness

Hao Yi[a], Weiquan Zhan[b], Yunliang Zhao[b,c,*], Xian Zhang[b], Feifei Jia[a], Wei Wang[b], Zhong Ai[b], Shaoxian Song[a,**]

[a] Hubei Key Laboratory of Mineral Resources Processing and Environment, Wuhan University of Technology, 122 Luoshi Road, Wuhan, Hubei, 430070, China
[b] School of Resources and Environmental Engineering, Wuhan University of Technology, 122 Luoshi Road, Wuhan, Hubei, 430070, China
[c] Materials Research Institute, The Pennsylvania State University, University Park, PA, 16802, USA

ARTICLE INFO

Keywords:
Two-dimensional montmorillonite nanosheet
Latent heat capacity
Shape-stabilized phase change material
Thermal transfer ability
Microcapsule

ABSTRACT

Clay minerals are excellent supporting materials to synthesize shape-stabilized phase change materials (ssPCMs) because of outstanding pore structure, excellent thermal stability, perfect organic compatibility and eco-friendly features. However, previous clay-based ssPCMs show very low thermal energy storage capacity due to little loading of working PCMs (< 65 wt%). In this work, stearic acid (SA) encapsulated by two-dimensional montmorillonite nanosheets (MtNS) has been designed in order to form core-shell structural MtNS/SA composite PCMs with ultra-high core mass fraction and dramatic latent heat capacity. This study mainly investigates the effect of MtNS shell thickness on thermal energy storage performances, including latent heat, thermal transfer ability, shape stability and cycling performances. Self-assembly mechanism of MtNS/SA was attributed to that the positively charged MtNS strongly attached on the surface of negatively charged SA latex particles and formed a core-shell structure mainly through electrostatic interaction. The MtNS/SA composite showed very large latent heat capacity (184.88 J/g) due to encapsulation of massive SA (> 85 wt%). Besides, the composite PCMs also displayed improved thermal transfer ability due to the combination of MtNS, which leads to outstanding thermal charging/discharging rate and excellent photo-thermal conversion efficiency. It was also found that the thinner the MtNS, the better the thermal conductivity and latent heat storage capacity. In addition, the MtNS/SA composites show thermal and structural stability, no leakage occurred even under the encapsulation of the thinnest MtNS shell. Also, the cycling performances of this composite PCMs are very outstanding owing to the effective protection of MtNS shell. Hence, this non-leaking and green MtNS/SA composite PCMs with high-performance heat storage properties can be applied in sustainable energy field.

1. Introduction

In recent years, green and pollution-free energy have attracted extensive interests due to energy crisis and environmental pollution [1]. Due to almost constant phase transition temperature and huge latent heat storage density, phase change materials (PCMs) can store and release tremendous latent heat during phase change process [2]. Hence, PCMs can provide a quick and facile way to solve the problems that energy supply does not match the demand in time and space [3,4]. As a result, PCMs has been strongly encouraged in recent decades and utilization of PCMs in various fields has been investigated. For example, in solar energy storage, PCMs can store inexhaustible and non-polluting solar energy thus to decrease the building energy consumption required for air conditioning, refrigeration, water heating and so on [5]. Besides, PCMs have potentials in recovering and reusing industrial waste heat which will contribute to low-carbon and free energy resource [6]. PCMs also provide a proper operating temperature and good thermal management system for some electronic components such as Li-ion batteries and photovoltaic cells [7–10]. In addition, PCMs can also played important role in smart textiles, medical application, thermo-regulating fibers and so on [11–13]. Therefore, PCMs show great promises in making full use of cleaner solar energy, saving energy, decreasing CO_2 emissions and relieving the currently energy crisis.

However, PCMs generally suffer from leakage during the solid to

* Corresponding author. School of Resources and Environmental Engineering, Wuhan University of Technology, 122 Luoshi Road, Wuhan, Hubei, 430070, China.
** Corresponding author.
E-mail addresses: zyl286@whut.edu.cn (Y. Zhao), ssx851215@whut.edu.cn (S. Song).

https://doi.org/10.1016/j.solmat.2019.109935
Received 14 March 2019; Received in revised form 7 May 2019; Accepted 8 May 2019
Available online 15 May 2019
0927-0248/

liquid phase transition process, which seriously limits the large-scale applications of PCMs [14]. In order to overcome the leakage problems, some supporting materials have to be used to prepare shape-stabilized phase change materials (ssPCMs) thus to prevent leakage during melting. Clay minerals are natural abundant, inexpensive and pollution-free materials which has been widely used in building materials, ceramics, papermaking, rubber and so on [15]. Besides, clay minerals are generally characterized by considerable porous structure, excellent absorbability and environmental friendly, which is considered as perfect supporting materials for synthesizing ssPCMs [16]. And various clay based composite PCMs has been reported in large volumes. Halloysite nanotubes are composed of multiple rolled layers consisting of hollow cylinders with sub-micrometer dimensions, into which PCMs can be easily encapsulated without leakage, the loading ratio of various PCMs are in the range of 20.1%–42.3% [17]. Organic PCMs were absorbed into the interlayer of kaolinite thus to synthesize ssPCMs and the maximum content of organic PCMs intercalated into kaolinite interlayer was 48 wt% [18–20]. Besides, intercalation of n-hecadecane into the interlayer structure of Na-montmorillonite has been prepared to show latent heat of 126 J/g with the PCMs mass ration of 60% [21]. Sepiolite supported stearic acid PCMs composite has also been designed with a 60% loading of PCMs and shows the thermal energy storage capacity of 118.7 J/g [22]. And diatomite with highly porous structure was used as carriers for Poly-ethylene glycols (PEG) and the latent heat capacity is 111.3 J/g with maximum PEG loading of 63% [23]. Though all kinds of clay-based composite PCMs has been developed, the thermal energy storage capacity of these composite PCMs are a little low due to the limited pore volume and limited loading ratio of PCMs.

Therefore, composite PCMs remain form-stability while present high content of active PCM materials at the same time is desperately needed before they can be largely applied in practical applications. Thus a high-performance ssPCMs with high active PCM materials and huge latent heat capacity have been attempted to developed in this work. Considering that montmorillonite is a layered aluminosilicate mineral and can be easy to exfoliated into two dimensional nanosheets (MtNS) due to swelling property [24–26], using these MtNS to encapsulate PCM and prepare clay based microencapsulated PCMs may greatly improve the active PCM content due to the ultra-thin shell thickness. Actually, the microencapsulation technology has been already widely used in composite PCMs in order to minimize PCM leakage [27]. However, the commonly used polymer shell materials had poor thermal stability, and the mass ratio of core PCMs materials is often not very high because a thick polymer shell is essential to effectively prevent leakage [28]. Recently developed graphene and related two-dimensional materials has also introduced into preparation of ssPCMs [29,30]. And the graphene based composite PCMs shows very good thermal storage properties, but the difficult exfoliation method and the high price of graphene based materials seriously limited the practical application of graphene based PCMs at large scale [31]. In comparison, the Mt with abundant reserves and very low price can be easily exfoliated into MtNS just through physical ultrasonic method [32], the MtNS based composite PCMs with superior thermal storage properties and low cost may show great promise in practical application because clay mineral is very commonly used building materials and other raw industrial materials originally.

In consequence, the purpose of this study is to introduce a facile way to synthesize microcapsule PCMs by using MtNS to encapsulate SA, and to solve the leakage, low content of active core materials, low thermal conductivity and high cost problem at the same time. The influences of MtNS shell thickness on latent heat capacity, thermal transfer ability and stability property of MtNS/SA composite PCMs has been investigated. The MtNS/SA composite PCMs with dramatic thermal energy storage capacity, improved thermal transfer ability, outstanding cycling performances, non-leaking and eco-friendly feature will show enormous potential in solar thermal energy storage, waste industrial thermal energy cycling and other sustainable energy fields.

2. Experiments

2.1. Materials

Natural montmorillonite (Mt) was used to prepare two dimensional montmorillonite nanosheets (MtNS), which were applied as shell materials of microcapsule PCMs. Stearic acid (SA) were used as working phase change materials. Hexadecyl trimethyl ammonium bromide (CTAB) is a very commonly used cationic surfactant, which is used to modify the negatively charged MtNS and to induce positive charge on MtNS surface. As common anionic surfactants, sodium dodecyl sulfate (SDS) were used to stabilize the SA latex particles and to enable the SA latex particles negatively surface charge. All these reagents with analytical purity were purchased from Sinopharm Chemical Reagent Company Limited in China.

2.2. Exfoliation of montmorillonite

The montmorillonite was exfoliated into nanosheets by ultrasonic as well as shearing treatments, and the details were shown in previous study [33]. Mt suspension was treated by a Vernon Hills Illinois CP505 ultrasonic dispersion instrument for 4 min in order to exfoliate the Mt layers, and different ultrasonic strength were chosen to exfoliate the montmorillonite and produce montmorillonite nanosheets with different thickness. The MtNS exfoliated at 150 W, 300 W and 450 W ultrasonic intensity were named MtNS-150, MtNS-300 and MtNS-450, respectively.

2.3. Self-assemble of MtNS and SA latex particles

The MtNS/SA composite PCMs were designed to self-assemble through electrostatic interactions. Thus the MtNS and SA latex particles have to be modified to be oppositely charged at first. MtNS (1.5 g) and CTAB (1.5 g) were dispersed in water (300 mL) and formed the modified MtNS suspensions after being stirred for 1 h. While SA (15 g) and SDS (1.5 g) were added to aqueous solution (100 mL) and heated to 90 °C, after being stirred for 3 h and then cool down, the solution of SA latex particles with negative surface charge could be prepared. Finally, MtNS/CTAB suspension and SA/SDS suspension were mixed and being stirred for 1 h, after which the MtNS/SA microcapsule PCMs would be formed by way of self-assembly. These finally resulted MtNS/SA composite PCMs were fully washed by ultrapure water and dried at 50 °C in vacuum. In order to investigate the effect of MtNS thickness on the thermal properties of MtNS/SA composite PCMs, MtNS with different thickness (MtNS-150, MtNS-300 and MtNS-450) have been used to prepare MtNS/SA composite PCMs with different shell thickness, and the resulted composite PCMs were called MtNS-150/SA, MtNS-300 and MtNS-450/SA, respectively.

2.4. Characterizations

Multimode 8 atomic force microscope (AFM) (Bruker, Germany) were used to determine the thickness of MtNS exfoliated by different ultrasonic intensity. The thickness of 250 exfoliated MtNS were obtained to measure thickness distribution of MtNS. Zeta potential measurements were carried out to determine the zeta potential of MtNS and SA, thus to analyze interaction mechanism between MtNS and SA latex particles [34]. Fourier transform infrared spectroscopy (FTIR) (Thermo Nicolet, US) were performed to investigate the interaction between MtNS and SA latex particles. Besides, scanning electronic microscope (SEM) (Zeiss Uitra 55, Germany) were used to observe the morphology of MtNS/SA composite PCMs. Differential scanning calorimeter (DSC) (PE 8500, US) has been applied for the measurement of latent heat capacity and phase change properties of MtNS/SA composite PCMs, these DSC measurements were performed at a heating rate of 1 °C/min ranged from 30 °C to 85 °C under N_2 atmosphere. And TPS2500S

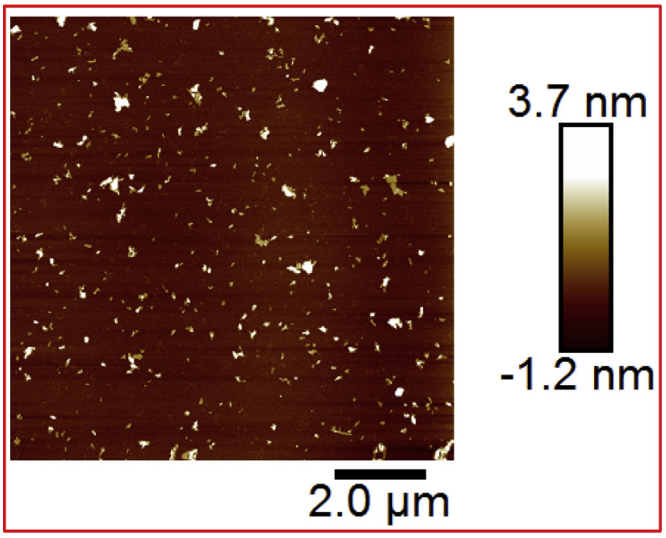

Fig. 1. AFM image of MtNS-300.

thermal constant analyzer (Hot Disk, Sweden) has been used to determine the thermal conductivity of MtNS/SA composite PCMs. As for the cycle stability, the MtNS/SA composites were heated in oven (90 °C) and then cooled in air to room temperature, the DSC measurements will be performed for this sample after 50 times heating/cooling cycling.

3. Results and discussion

3.1. Exfoliation of montmorillonite

To characterize the exfoliation degree of Mt, AFM images of MtNS have been captured to observe the thickness of MtNS. Fig. 1 gives the AFM images of MtNS exfoliated with ultrasonic intensity of 300 W and shows that the thickness of MtNS are only several nanometers. These observed nanosheets in the AFM image demonstrate the successful exfoliation of Mt and the successful preparation of MtNS. In order to representatively assess the exfoliation degree of Mt under different ultrasonic intensity, thickness of 250 montmorillonite nanosheets have been determined to analyze the thickness distribution of MtNS. As shown in Fig. 2, 8.7% of the MtNS-150 are in thickness of 1-2 nm when exfoliated under 150 W ultrasonic intensity (Fig. 2a), while it increases to 56% when exfoliated under 450 W ultrasonic intensity (Fig. 2c). It is known that the thickness of Mt monolayer is around 1 nm, thus most of Mt are being exfoliated into Mt monolayer under 450 W ultrasonic strength. Besides, the average thickness of MtNS are decreased with the enhancement of ultrasonic intensity. Thus, the MtNS-450 exfoliated at 450 W ultrasonic strength shows the thinnest thickness while the MtNS-150 shows the relatively thicker thickness.

3.2. Self-assembly of MtNS and SA latex particle

The MtNS/SA composite PCMs were designed to self-assemble and form a core-shell structure with MtNS shell and SA core. To verify this hypothesis, SEM images of MtNS/SA composites has been obtained to observe the morphology. As shown in Fig. 3a–b, the MtNS/SA composite PCMs are in shape of globule with average size of around a dozen microns. In addition, it is clearly to see that the SA particle are tightly wrapped by the ultra-thin MtNS. These flake-like MtNS covered the SA on the core surfaces turned out that the MtNS/SA composite PCMs are microcapsule products with core-shell structure. These SEM images have successfully demonstrated that SA latex particles are encapsulated by montmorillonite nanosheets. Thus, a simple mixting of MtNS and SA latex enable the self-assembly of MtNS on SA latex particles surface, which provides an easy and fast way to prepare shape-stabilized

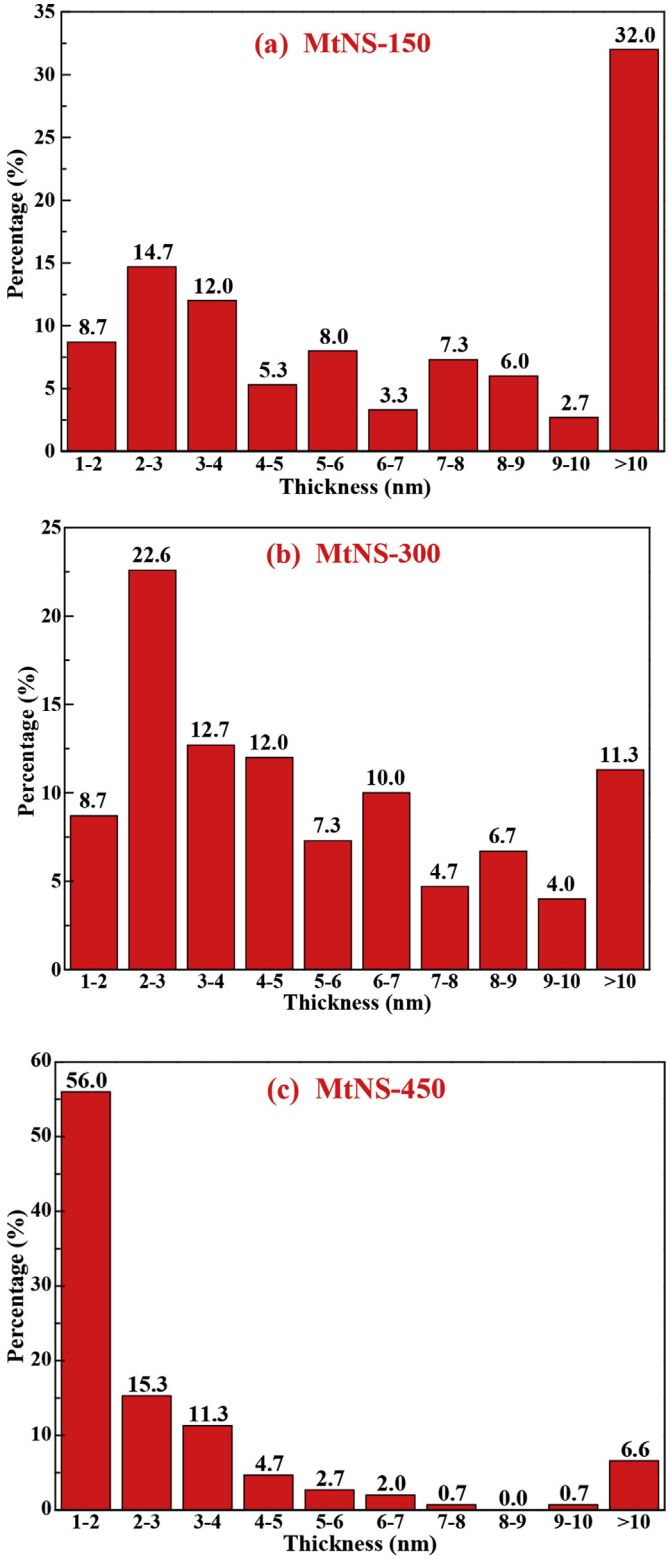

Fig. 2. Thickness distribution of MtNS-150 (a), MtNS-300 (b) and MtNS-450 (c).

composite PCMs with core-shell structure. And the MtNS shell encapsulated on SA surface provides well-defined MtNS framework wrapping SA latex particles inside, which contributes to stabilize the shape of MtNS/SA composite PCMs and is beneficial to prevent leakage during phase change process.

In order to investigate the self-assembly mechanism between MtNS

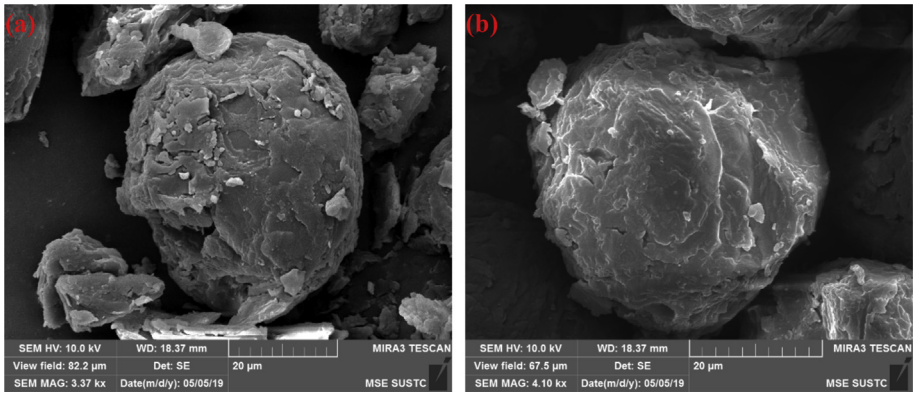

Fig. 3. SEM image of MtNS-300/SA composite PCMs.

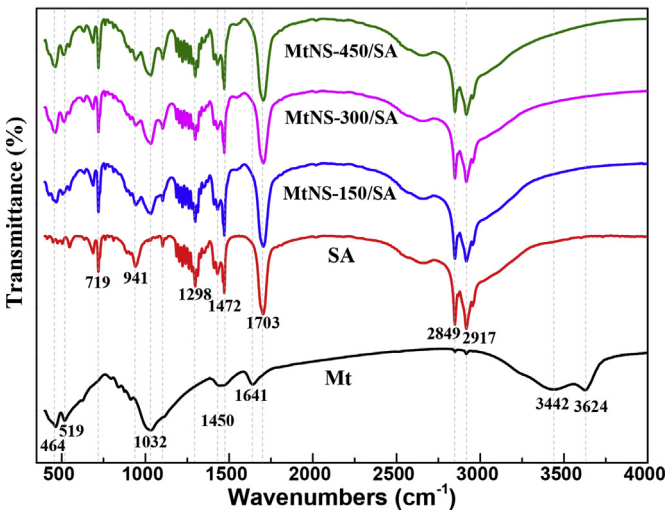

Fig. 4. FTIR spectrograms of MtNS, SA and MtNS/SA composite PCMs.

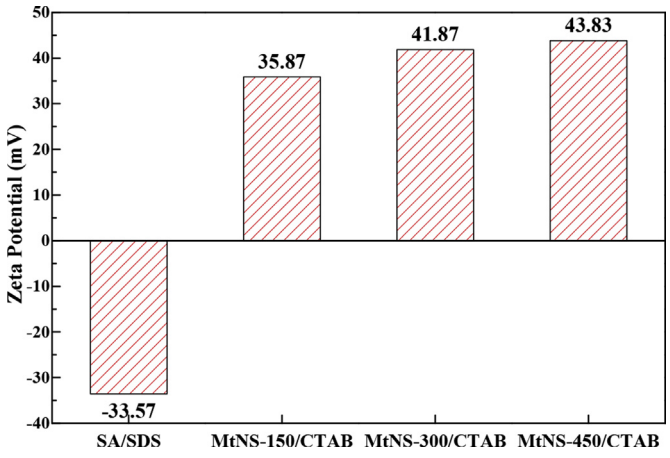

Fig. 5. Zeta potential of SA/SDS and MtNS/CTAB.

and SA, FTIR has been used to determine the interactions between MtNS and SA. Fig. 4 shows the FTIR spectrograms of MtNS, SA and MtNS/SA composite PCMs. In the FTIR spectrograms of Mt [25,35,36], 3624 cm^{-1} was due to the stretching vibration of –OH in Mt structure, 3442 cm^{-1} and 1641 cm^{-1} are considered as stretching and bending vibrations of –OH in hydration water molecules. Besides, 1032 cm^{-1} and 464 cm^{-1} were attributed to the vibration of Si–O bonds, 519 cm^{-1} is caused by the bending stretching of Al–O–Si. With regard to SA [37], the peaks at 2917 cm^{-1} and 2849 cm^{-1} are caused by the stretching vibration of C–H, and the peaks at 1703 cm^{-1} and 1472 cm^{-1} are due to the carboxylic acid stretching vibration (C = O) and symmetric carboxyl stretching vibration (COO-), respectively. Besides, 1298 cm^{-1} and 942 cm^{-1} belong to the bending vibration of –OH group while 719 cm^{-1} corresponds to the vibration of $–CH_2$ group. In the spectra of MtNS/SA composite PCMs, it is clear that the main absorption peaks at 719, 941, 1298, 1472, 1703, 2849 and 2917 cm^{-1} are similar to that of pure SA while 464, 519 and 1032 cm^{-1} are belonging to the groups in MtNS structure. Thus, the occurrences of both absorption bands from SA and MtNS determined the successful combination of MtNS and SA. In addition, no absorption bands shift suggests that SA and MtNS are compound just through physical interactions.

For the sake of exploring the detailed combination mechanism, zeta potentials of SA latex particles and modified MtNS has been measured, as shown in Fig. 5. It should be noted that SA latex particles present a very negative surface charge (−33.57 mV) while the MtNS show very positive surface charge. And the thinner the MtNS, the more positive surface charge of the modified MtNS. Considering the opposite surface charge of MtNS and SA latex particles, it is evident that there is very strong electrostatic attraction between the negatively charged SA and the positively charged MtNS. Thus, it can be concluded that the MtNS and SA latex particles are self-assembled mainly through electrostatic interactions. Compared with previous study, some other interactions such as hydrogen bond interaction and hydrophobic attractions may also exist between the MtNS and SA latex particles [38]. To sum up, the strong electrostatic interactions, the possible hydrogen bond and hydrophobic attractions results in the self-assemble of MtNS and SA and finally leads to formation of microcapsule composite PCMs with core-shell structure.

Based on the above analysis, the synthetic process and microstructure of MtNS/SA composite PCMs has been schematically illustrated in Fig. 6. Mt has been exfoliated and modified to be a two-dimensional montmorillonite nanosheet with positive surface charge, while SA were stabilized and modified by SDS to form negatively charged latex particles. After mixing, MtNS and SA latex particles electrostatically self-assemble to form microcapsule PCMs. Hydrogen bond interaction and hydrophobic attraction may also play an important role in the combination of MtNS and SA latex particles. The MtNS provides the possibility to trap SA inside and prevents the leakage effectively when SA were melted. Besides, MtNS shell materials with thinner thickness was believed to greatly enhance the mass fraction of SA core materials, thus to improve the latent heat storage. The thermal storage properties of MtNS/SA composite PCMs as affected by the shell thickness will be discussed in details in the next section.

3.3. Thermal energy storage capacity of MtNS/SA composite PCMs

Latent heat capacity is a very important index to evaluate the thermal property of composite PCMs [39], thus the DSC has been

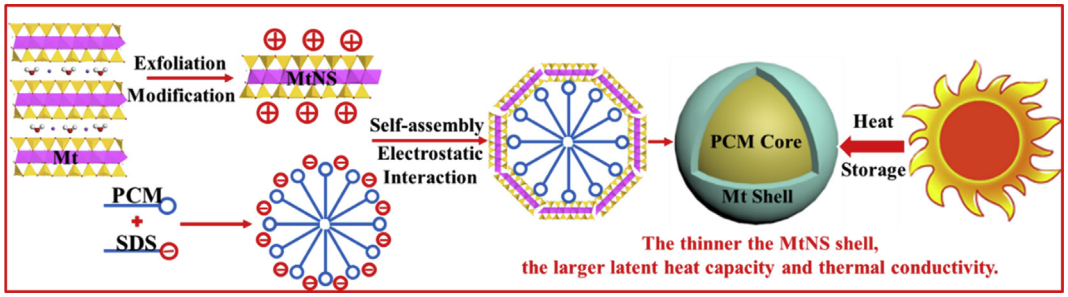

Fig. 6. Preparation process and self-assembly mechanisms of MtNS/SA composite PCMs.

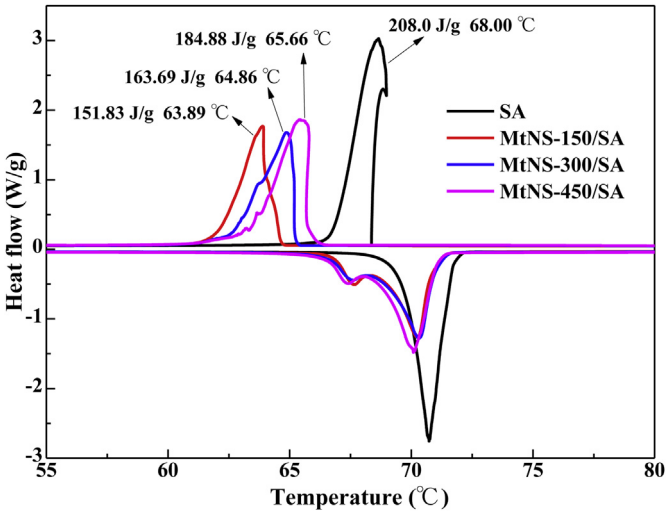

Fig. 7. DSC curves of pure SA and MtNS/SA composite PCMs.

measured to characterize the thermal energy storage property of MtNS/SA composite PCMs prepared in this work. Fig. 7 gives the DSC curves of pure SA and MtNS/SA composite PCMs. It is shown that the pure SA presents a latent heat capacity of 208.0 J/g, while the latent heat capacity of MtNS-450/SA, MtNS-300/SA and MtNS-150/SA are 184.88 J/g, 163.69 J/g and 151.83 J/g, respectively. MtNS occupy part of the volume of the composite PCMs, which leads to the decrease of thermal storage capacity of composite PCMs compared to pure PCM. As a result, the thinner thickness of the MtNS shell, the larger loading of SA and the larger the latent heat of composite PCMs. As can be calculated, the mass fraction of SA in MtNS-450/SA composite PCM is 88.88% according to Eq. (1), which are far larger than that of the two other composite PCMs (78.70% and 73.00%). Therefore, MtNS with thinner thickness will contribute to decrease the shell volume and increase the mass fraction of SA PCM, which leads to a relatively high latent heat capacity of MtNS/SA composite PCMs. It is noted that the MtNS/SA composite PCMs showed more serious supercooling phenomenon, which may be caused by the interface thermal resistance between the montmorillonite nanosheet and the stearic acid [40,41].

$$\eta = \frac{\Delta H_{MtNS/SA}}{\Delta H_{SA}} \times 100\% \quad (1)$$

where η is the weight fraction of SA in the MtNS/SA PCM composites, $\Delta H_{MtNS/SA}$ is the latent heat of MtNS/SA composite PCMs and the ΔH_{SA} is the latent heat of pure SA.

In order to quantitatively express the excellent latent heat performance of MtNS/SA composite PCMs, some previous research on clay minerals based ssPCMs have been cited and comparatively analyzed. Various clay minerals based composite PCMs with relatively high load capacity of pure PCM has been listed in Table 1, it is obvious that MtNS/SA composite prepared in this work has significant advantages in the PCM loading capacity due to the ultra-thin shell. Commonly used clay minerals shows the maximum loading ratio of 66.1 while MtNS can load 88.88% of SA at most in this study. A huge improvement of the mass fraction of PCM will beneficial to greatly improve the latent heat capacity, which significantly contributes to the enhancement of thermal energy storage properties.

Table 1
Latent heat of MtNS/SA and previous reported clay/SA ssPCMs.

Clay based composite PCMs	Mass fraction of PCM (%)	References
Perlite based composite PCMs	60.0	[42]
Sepiolite based composite PCMs	60.0	[22]
Vermiculite based composite PCMs	66.1	[43,44]
Kaolinite based composite PCMs	44.95	[19]
Diatomite based composite PCMs	63.0	[23,45]
Montmorillonite based composite PCMs	60	[21,46]
MtNS/SA	**88.88**	**This work**

3.4. Thermal conductivity of MtNS/SA composite PCMS

PCMs have huge promising as advanced thermal energy storage technique if the thermal transfer ability is good enough, which determines the thermal charging/discharging rate [47]. Herein, thermal conductivity has also been measured to assess the heat transfer rate of the MtNS/SA. Fig. 8 shows the thermal conductivity of SA, MtNS with different thickness and MtNS/SA composite PCMs prepared by MtNS with different thickness. It is shown that the thermal conductivity of SA is very low (0.20 W/mK), while the thermal conductivity of MtNS is relatively high compared with that of SA. Besides, the thermal conductivity of MtNS are increasing with the decrease of thickness. It is clearly to see that the thermal conductivity of MtNS-150 is 0.35 W/mK while that value of MtNS-450 is 0.46 W/mK. Thus the MtNS with

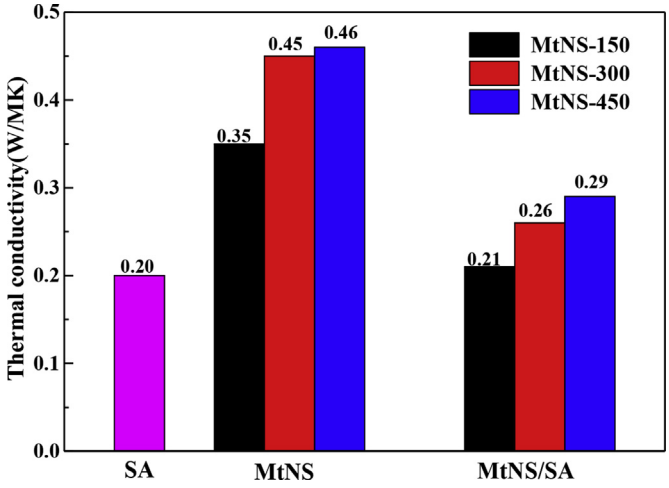

Fig. 8. Thermal conductivity of MtNS, SA and MtNS/SA composite PCMs.

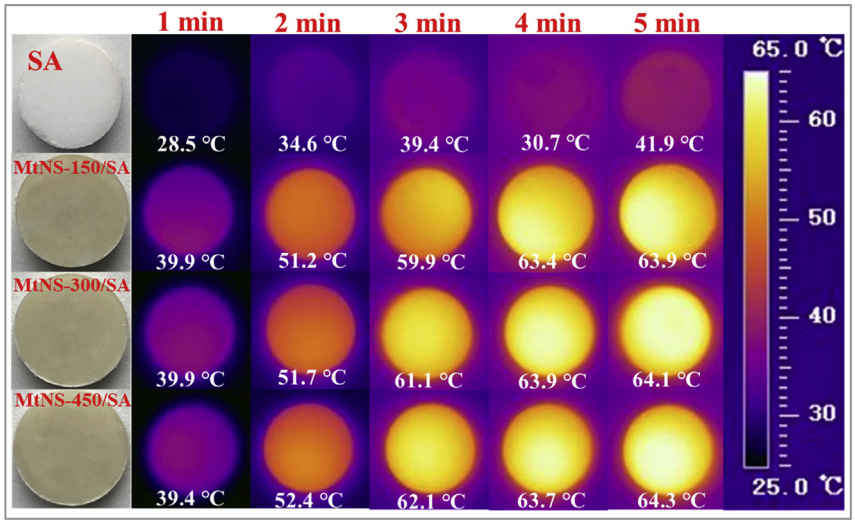

Fig. 9. Infrared camera images of SA and MtNS/SA composite PCMs under sun simulator.

thinner thickness and relatively higher thermal conductivity can contribute to the improvement of thermal conductivity of MtNS/SA composite PCMs. As expected, the MtNS/SA prepared by much thinner MtNS shows a much higher thermal conductivity (0.29 W/mK), this value presents a huge improvement in thermal conductivity compared with that of pure SA (0.20 W/mK). In conclusions, MtNS with much thinner thickness not only contribute to a larger latent heat capacity, but also do good to the enhancement of heat transfer rate of composite PCMs.

3.5. Photo-thermal conversion performances of MtNS/SA composite PCMS

Solar energy conversion to thermal energy is one of the most efficient methods to take advantage of the most abundant renewable solar energy [48]. However, the low thermal conductivity and low photo-thermal conversion efficiency are major drawbacks. Due to the combination of MtNS with improved thermal transfer ability, the solar energy to thermal energy conversion are supposed to be promoted greatly due to the significant enhancement of thermal transfer ability. As shown in Fig. 9, the temperature of pure SA only increase to 41.9 °C from 28.5 °C under solar radiation for 5 min, which suggests the bad thermal transfer ability of SA and the poor photo-thermal conversion efficiency. After combination of MtNS, the thermal transfer ability has been greatly promoted. Only irradiate for 3 min, temperature of MtNS/SA composite PCMs increase to 59.9 °C, 61.1 °C and 62.1 °C, indicating the rapid thermal transfer ability of composite PCMs. After 3 min solar radiation, the temperatures of composite PCMs are close to the phase change temperature, and PCMs will undergo solid-liquid phase change and store massive thermal energy in this case. Thus, it is reasonable that the temperature increase of composite PCMs become slow after 3 min sun radiation. Compare to the pure SA, all the composite PCMs shows much faster thermal transfer ability, leading the MtNS/SA composite PCMs to excellent photo-thermal conversion performances. Besides, the rapid temperature increase of composite PCMs turns out the fast thermal charging rate, which enables this composite PCMs the direct solar energy storage and utilization.

3.6. Shape stability of MtNS/SA composite PCMs

Structure and thermal stability test has been carried out in this section, and Fig. 10 gives the photographs of SA and MtNS/SA composite PCMs on a hot plate at 85 °C. From these photographs, it is obvious that the SA melt to liquid quickly when the temperature exceeds the melting point. On the other hand, the SA encapsulated by MtNS maintains a very stable shape even the temperature is far higher than the melting point of SA (~70 °C). That no leakage occurred demonstrated all the MtNS/SA composite PCMs, no matter encapsulated by a thinner or a thicker shell, are shape-stabilized. The thermal stable MtNS shell retain the shape of MtNS/SA composite PCMs even SA were melted. Besides, the MtNS provides a framework to prevent the leakage of melted SA. This simple heating test suggests that MtNS is an excellent shell material to encapsulate the PCM thus to keep the shape and prevent the leakage of composite PCMs. In summary, the MtNS/SA composite PCMs with MtNS shell and SA core is form-stabilized, because the MtNS trapped SA inside effectively thus to prevent SA from leakage when melted.

3.7. Cycling performance of MtNS/SA composite PCMs

Stable heating/cooling cycling performances of composite PCMs are also a key issue when put into real applications [49]. Fig. 11 shows the DSC curves of MtNS/SA composite PCMs before and after 50 heating/cooling cycles. The latent heat capacity of MtNS-300/SA before and after heat/cooling cycles is 166.21 J/g and 165.12 J/g, respectively. The phase change temperature of MtNS-300/SA composite PCMs is 69.36 °C and 69.51 °C, respectively. Only very slight changes of the thermal storage capacity and phase change temperature has occurred, which suggests that this composite PCMs shows excellent cycling performances in the charging/discharging tests. These negligible phase change properties after 50 times cycling almost have no influences on the practical application of MtNS/SA. Thus MtNS/SA composite displays a stable cycling performance, which also demonstrates the shape stability of MtNS/SA composite PCMs.

To sum up, Mt are natural clay minerals with abundant reserves and very low prices. Besides, Mt can be easily exfoliated into MtNS just by ultrasonication due to the swelling property. Through modification, the MtNS and SA latex particles self-assemble to form microcapsule PCMs with a core-shell structure under the electrostatic interactions, hydrogen bond interaction and hydrophobic attraction may also work in this process. MtNS/SA displays relatively high thermal conductivity, ultra-high thermal storage capacity, outstanding photo-thermal conversion performances, perfect cycling performances and excellent shape stability, which enables this composite PCMs significant potential in solar thermal energy storage, building energy cycle, industrial waste heat recovering and other renewable energy utilization.

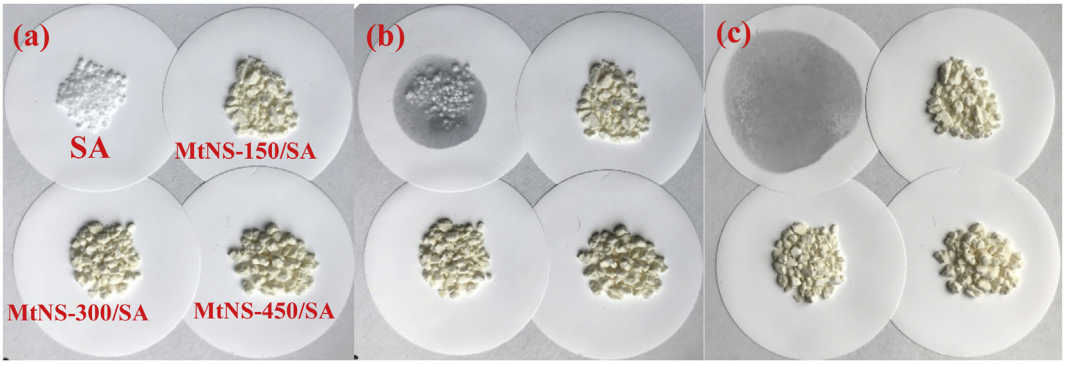

Fig. 10. Structural stability test of MtNS/SA composite PCMs.

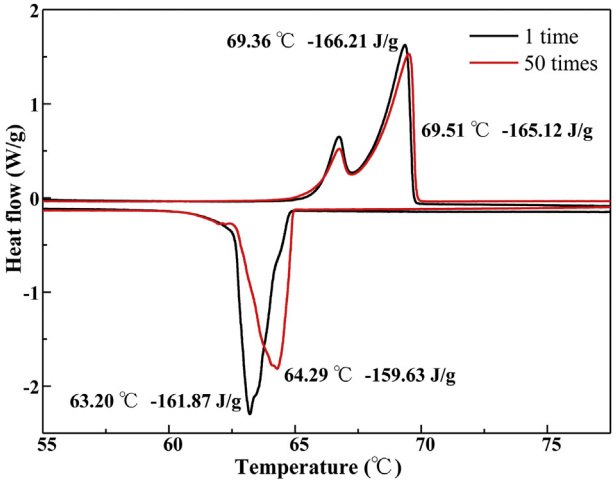

Fig. 11. DSC curves of MtNS-300/SA composite PCMs before and after 50 heating/cooling cycles.

4. Conclusions

(1) Two-dimensional montmorillonite nanosheets are excellent supporting materials for preparing shape-stabilized phase change materials due to excellent thermal properties and very low price.
(2) The thinner the thickness of the MtNS, the more negative surface charge of MtNS after surface modification, and the stronger electrostatic interaction in the self-assembly of MtNS and SA.
(3) The thinner the thickness of MtNS, the larger SA mass ratio in the MtNS/SA composite PCMs and the larger latent heat capacity.
(4) The thermal transfer ability of MtNS/SA composite PCMs are increasing with the decrease of the MtNS thickness.
(5) MtNS/SA composite PCMs show excellent photo-thermal conversion efficiency and dramatic thermal charging/discharging rate.
(6) MtNS/SA composite PCMs prepared by the thinnest MtNS still shows outstanding shape stability and perfect cycling performances.
(7) The MtNS/SA composite shows huge potential in sustainable energy field due to the ultra-high latent heat capacity, perfect shape stability and superior cycling performances.

Acknowledgements

The financial from the National Natural Science Foundation of China (51674183 and 51874220) supports to this work are gratefully acknowledged. Natural Science Foundation of Hubei Province of China (2018CFB468) has also supported this research.

Appendix A. Supplementary data

Supplementary data to this article can be found online at https://doi.org/10.1016/j.solmat.2019.109935.

References

[1] Y. Chen, Q. Zhang, X. Wen, H. Yin, J. Liu, A novel CNT encapsulated phase change material with enhanced thermal conductivity and photo-thermal conversion performance, Sol. Energy Mater. Sol. Cells 184 (2018) 82–90, https://doi.org/10.1016/j.solmat.2018.04.034.
[2] W. Wang, B. Tang, B. Ju, Z. Gao, J. Xiu, S. Zhang, Fe $_3$ O $_4$ -functionalized graphene nanosheet embedded phase change material composites: efficient magnetic- and sunlight-driven energy conversion and storage, J. Mater. Chem. A. 5 (2017) 958–968, https://doi.org/10.1039/C6TA07144A.
[3] A.A. Aydin, A. Aydin, High-chain fatty acid esters of 1-hexadecanol for low temperature thermal energy storage with phase change materials, Sol. Energy Mater. Sol. Cells 96 (2012) 93–100, https://doi.org/10.1016/j.solmat.2011.09.013.
[4] Z. Ling, J. Liu, Q. Wang, W. Lin, X. Fang, Z. Zhang, MgCl2·6H2O-Mg(NO3)2·6H2O eutectic/SiO2composite phase change material with improved thermal reliability and enhanced thermal conductivity, Sol. Energy Mater. Sol. Cells 172 (2017) 195–201, https://doi.org/10.1016/j.solmat.2017.07.019.
[5] C. Chen, H. Ling, Z.(John, Zhai, Y. Li, F. Yang, F. Han, S. Wei, Thermal performance of an active-passive ventilation wall with phase change material in solar greenhouses, Appl. Energy 216 (2018) 602–612, https://doi.org/10.1016/j.apenergy.2018.02.130.
[6] L. Miró, J. Gasia, L.F. Cabeza, Thermal energy storage (TES) for industrial waste heat (IWH) recovery: a review, Appl. Energy 179 (2016) 284–301, https://doi.org/10.1016/j.apenergy.2016.06.147.
[7] F. Samimi, A. Babapoor, M. Azizi, G. Karimi, Thermal management analysis of a Li-ion battery cell using phase change material loaded with carbon fibers, Energy 96 (2016) 355–371, https://doi.org/10.1016/j.energy.2015.12.064.
[8] Z. Ling, Z. Zhang, G. Shi, X. Fang, L. Wang, X. Gao, Y. Fang, T. Xu, S. Wang, X. Liu, Review on thermal management systems using phase change materials for electronic components, Li-ion batteries and photovoltaic modules, Renew. Sustain. Energy Rev. 31 (2014) 427–438, https://doi.org/10.1016/j.rser.2013.12.017.
[9] P. Goli, S. Legedza, A. Dhar, R. Salgado, J. Renteria, A.A. Balandin, Graphene-enhanced hybrid phase change materials for thermal management of Li-ion batteries, J. Power Sources 248 (2014) 37–43, https://doi.org/10.1016/j.jpowsour.2013.08.135.
[10] Y. Wang, H. Mi, Q. Zheng, Z. Ma, S. Gong, Graphene/phase change material nanocomposites: light-driven, reversible electrical resistivity regulation via form-stable phase transitions, ACS Appl. Mater. Interfaces 7 (2015) 2641–2647, https://doi.org/10.1021/am507700r.
[11] Y. Cai, H. Ke, L. Lin, X. Fei, Q. Wei, L. Song, Y. Hu, H. Fong, Preparation, morphology and thermal properties of electrospun fatty acid eutectics/polyethylene terephthalate form-stable phase change ultrafine composite fibers for thermal energy storage, Energy Convers. Manag. 64 (2012) 245–255, https://doi.org/10.1016/j.enconman.2012.04.018.
[12] Y. Lin, Y. Jia, G. Alva, G. Fang, Review on thermal conductivity enhancement, thermal properties and applications of phase change materials in thermal energy storage, Renew. Sustain. Energy Rev. 82 (2018) 2730–2742, https://doi.org/10.1016/j.rser.2017.10.002.
[13] K. Du, J. Calautit, Z. Wang, Y. Wu, H. Liu, A review of the applications of phase change materials in cooling, heating and power generation in different temperature ranges, Appl. Energy 220 (2018) 242–273, https://doi.org/10.1016/j.apenergy.2018.03.005.
[14] Y. Xu, A.S. Fleischer, G. Feng, Reinforcement and shape stabilization of phase-change material via graphene oxide aerogel, Carbon N. Y. 114 (2017) 334–346, https://doi.org/10.1016/j.carbon.2016.11.069.
[15] F. Bergaya, G. Lagaly, Chapter 1 general introduction: clays, clay minerals, and clay science, Dev. Clay Sci. 1 (2006) 1–18, https://doi.org/10.1016/S1572-4352(05)01001-9.

[16] P. Lv, C. Liu, Z. Rao, Review on clay mineral-based form-stable phase change materials: preparation, characterization and applications, Renew. Sustain. Energy Rev. 68 (2017) 707–726, https://doi.org/10.1016/j.rser.2016.10.014.
[17] W. Liang, Y. Wu, H. Sun, Z. Zhu, P. Chen, B. Yang, A. Li, Halloysite clay nanotubes based phase change material composites with excellent thermal stability for energy saving and storage, RSC Adv. 6 (2016) 19669–19675, https://doi.org/10.1039/C5RA27964J.
[18] S. Liu, H. Yang, Composite of coal-series kaolinite and capric-lauric acid as form-stable phase-change material, Energy Technol. 3 (2015) 77–83, https://doi.org/10.1002/ente.201402125.
[19] S. Song, L. Dong, Y. Zhang, S. Chen, Q. Li, Y. Guo, S. Deng, S. Si, C. Xiong, Lauric acid/intercalated kaolinite as form-stable phase change material for thermal energy storage, Energy 76 (2014) 385–389, https://doi.org/10.1016/j.energy.2014.08.042.
[20] S. Liu, H. Yang, Stearic acid hybridizing coal-series kaolin composite phase change material for thermal energy storage, Appl. Clay Sci. 101 (2014) 277–281, https://doi.org/10.1016/j.clay.2014.09.002.
[21] N. Sarier, E. Onder, S. Ozay, Y. Ozkilic, Preparation of phase change material-montmorillonite composites suitable for thermal energy storage, Thermochim. Acta 524 (2011) 39–46, https://doi.org/10.1016/j.tca.2011.06.009.
[22] Q. Shen, S. Liu, J. Ouyang, H. Yang, Sepiolite supported stearic acid composites for thermal energy storage, RSC Adv. 6 (2016) 112493–112501, https://doi.org/10.1039/C6RA22015K.
[23] T. Qian, J. Li, X. Min, W. Guan, Y. Deng, L. Ning, Enhanced thermal conductivity of PEG/diatomite shape-stabilized phase change materials with Ag nanoparticles for thermal energy storage, J. Mater. Chem. A. 3 (2015) 8526–8536, https://doi.org/10.1039/C5TA00309A.
[24] H. Yi, F. Jia, Y. Zhao, W. Wang, S. Song, H. Li, C. Liu, Surface wettability of montmorillonite (0 0 1) surface as affected by surface charge and exchangeable cations: a molecular dynamic study, Appl. Surf. Sci. 459 (2018) 148–154, https://doi.org/10.1016/j.apsusc.2018.07.216.
[25] S. Kang, Y. Zhao, W. Wang, T. Zhang, T. Chen, H. Yi, F. Rao, S. Song, Removal of methylene blue from water with montmorillonite nanosheets/chitosan hydrogels as adsorbent, Appl. Surf. Sci. 448 (2018) 203–211, https://doi.org/10.1016/j.apsusc.2018.04.037.
[26] T. Chen, Y. Yuan, Y. Zhao, F. Rao, S. Song, Preparation of montmorillonite nanosheets through freezing/thawing and ultrasonic exfoliation, Langmuir 35 (2019) 2368–2374, https://doi.org/10.1021/acs.langmuir.8b04171.
[27] C. Liu, Z. Rao, J. Zhao, Y. Huo, Y. Li, Review on nanoencapsulated phase change materials: preparation, characterization and heat transfer enhancement, Nano Energy 13 (2015) 814–826, https://doi.org/10.1016/j.nanoen.2015.02.016.
[28] Z. Chen, J. Wang, F. Yu, Z. Zhang, X. Gao, Preparation and properties of graphene oxide-modified poly(melamine-formaldehyde) microcapsules containing phase change material n-dodecanol for thermal energy storage, J. Mater. Chem. A. 3 (2015) 11624–11630, https://doi.org/10.1039/C5TA01852H.
[29] T.D. Dao, H.M. Jeong, A Pickering emulsion route to a stearic acid/graphene core-shell composite phase change material, Carbon N. Y. 99 (2016) 49–57, https://doi.org/10.1016/j.carbon.2015.12.009.
[30] Y. Zhang, X. Zheng, H. Wang, Q. Du, Encapsulated phase change materials stabilized by modified graphene oxide, J. Mater. Chem. A. 2 (2014) 5304, https://doi.org/10.1039/c3ta15242a.
[31] L. Zhang, R. Li, B. Tang, P. Wang, Solar-thermal conversion and thermal energy storage of graphene foam-based composites, Nanoscale 8 (2016) 14600–14607, https://doi.org/10.1039/C6NR03921A.
[32] W. Wang, Y. Zhao, H. Bai, T. Zhang, V. Ibarra-Galvan, S. Song, Methylene blue removal from water using the hydrogel beads of poly(vinyl alcohol)-sodium alginate-chitosan-montmorillonite, Carbohydr. Polym. 198 (2018) 518–528, https://doi.org/10.1016/j.carbpol.2018.06.124.
[33] W. Wang, Y. Zhao, H. Yi, T. Chen, S. Kang, H. Li, S. Song, Preparation and characterization of self-assembly hydrogels with exfoliated montmorillonite nanosheets and chitosan, Nanotechnology 29 (2018), https://doi.org/10.1088/1361-6528/aa9ba4.
[34] T. Chen, Y. Zhao, S. Song, Electrophoretic mobility study for heterocoagulation of montmorillonite with fluorite in aqueous solutions, Powder Technol. 309 (2017) 61–67, https://doi.org/10.1016/j.powtec.2016.12.086.
[35] S.G. Jeong, S. Jin Chang, S. We, S. Kim, Energy efficient thermal storage montmorillonite with phase change material containing exfoliated graphite nanoplatelets, Sol. Energy Mater. Sol. Cells 139 (2015) 65–70, https://doi.org/10.1016/j.solmat.2015.03.010.
[36] Y. Cai, L. Song, Q. He, D. Yang, Y. Hu, Preparation, thermal and flammability properties of a novel form-stable phase change materials based on high density polyethylene/poly(ethylene-co-vinyl acetate)/organophilic montmorillonite nanocomposites/paraffin compounds, Energy Convers. Manag. 49 (2008) 2055–2062, https://doi.org/10.1016/j.enconman.2008.02.013.
[37] L. Liu, K. Zheng, Y. Yan, Z. Cai, S. Lin, X. Hu, Graphene Aerogels Enhanced Phase Change Materials prepared by one-pot method with high thermal conductivity and large latent energy storage, Sol. Energy Mater. Sol. Cells 185 (2018) 487–493, https://doi.org/10.1016/j.solmat.2018.06.005.
[38] T.D. Dao, H.M. Jeong, Novel stearic acid/graphene core-shell composite microcapsule as a phase change material exhibiting high shape stability and performance, Sol. Energy Mater. Sol. Cells 137 (2015) 227–234, https://doi.org/10.1016/j.solmat.2015.02.009.
[39] H. Yi, W. Zhan, Y. Zhao, S. Qu, W. Wang, P. Chen, S. Song, A novel core-shell structural montmorillonite nanosheets/stearic acid composite PCM for great promotion of thermal energy storage properties, Sol. Energy Mater. Sol. Cells 192 (2019) 57–64, https://doi.org/10.1016/j.solmat.2018.12.015.
[40] H. Ji, D.P. Sellan, M.T. Pettes, X. Kong, J. Ji, L. Shi, R.S. Ruoff, Enhanced thermal conductivity of phase change materials with ultrathin-graphite foams for thermal energy storage, Energy Environ. Sci. 7 (2014) 1185–1192, https://doi.org/10.1039/c3ee42573h.
[41] L.F. Cabeza, H. Mehling, S. Hiebler, F. Ziegler, Heat transfer enhancement in water when used as PCM in thermal energy storage, Appl. Therm. Eng. 22 (2002) 1141–1151, https://doi.org/10.1016/S1359-4311(02)00035-2.
[42] A. Karaipekli, A. Biçer, A. Sarı, V.V. Tyagi, Thermal characteristics of expanded perlite/paraffin composite phase change material with enhanced thermal conductivity using carbon nanotubes, Energy Convers. Manag. 134 (2017) 373–381, https://doi.org/10.1016/j.enconman.2016.12.053.
[43] Y. Deng, J. Li, T. Qian, W. Guan, Y. Li, X. Yin, Thermal conductivity enhancement of polyethylene glycol/expanded vermiculite shape-stabilized composite phase change materials with silver nanowire for thermal energy storage, Chem. Eng. J. 295 (2016) 427–435, https://doi.org/10.1016/j.cej.2016.03.068.
[44] W. min Guan, J. hong Li, T. ting Qian, X. Wang, Y. Deng, Preparation of paraffin/expanded vermiculite with enhanced thermal conductivity by implanting network carbon in vermiculite layers, Chem. Eng. J. 277 (2015) 56–63, https://doi.org/10.1016/j.cej.2015.04.077.
[45] T. Qian, J. Li, Octadecane/C-decorated diatomite composite phase change material with enhanced thermal conductivity as aggregate for developing structural–functional integrated cement for thermal energy storage, Energy 142 (2018) 234–249, https://doi.org/10.1016/j.energy.2017.10.021.
[46] K. Peng, L. Fu, X. Li, J. Ouyang, H. Yang, Stearic acid modified montmorillonite as emerging microcapsules for thermal energy storage, Appl. Clay Sci. 138 (2017) 100–106, https://doi.org/10.1016/j.clay.2017.01.003.
[47] X. Ma, Y. Liu, H. Liu, L. Zhang, B. Xu, F. Xiao, Fabrication of novel slurry containing graphene oxide-modified microencapsulated phase change material for direct absorption solar collector, Sol. Energy Mater. Sol. Cells 188 (2018) 73–80, https://doi.org/10.1016/j.solmat.2018.08.021.
[48] B. Tang, H. Wei, D. Zhao, S. Zhang, Light-heat conversion and thermal conductivity enhancement of PEG/SiO2 composite PCM by in situ Ti4O7 doping, Sol. Energy Mater. Sol. Cells 161 (2017) 183–189, https://doi.org/10.1016/j.solmat.2016.12.003.
[49] X. Huang, X. Chen, A. Li, D. Atinafu, H. Gao, W. Dong, G. Wang, Shape-stabilized phase change materials based on porous supports for thermal energy storage applications, Chem. Eng. J. 356 (2019) 641–661, https://doi.org/10.1016/j.cej.2018.09.013.